

# ELECTRO HYDRAULIC PRE-ACTUATOR MODELLING OF AN HYDRAULIC JACK

Salazar Garcia Mahuampy, Viot Philippe

Laboratoire Matériaux Endommagement Fiabilité et Ingénierie des Procédés (LAMEFIP), France

Nouillant Michel

Keywords: Three-stage servo-valve, modeling, hydraulic jack.

Abstract: Before the realization of testing devices such as a high speed (5m/s) hydraulic hexapod with a high load capacity (60 tons and 6 tons for static and dynamic operating mode), the simulation is an essential step. Hence from softwares such as SimMechanics, we have performed an electro hydraulic model of the servo-valve-jack part by using parameters and recorded results with mono axis testing bench of high-speed hydraulic jack (5m/s), which has a high loading capacity (10 tons for static and 1 ton for dynamic operating mode). The high-speed jack is provided by two parallel three-stage servo-valves. Each three-stage servo-valve supplies 600L/mm. Therefore the unit allows us to obtain a realistic model of an extrapolated hexapod from the mono axis currently used. The aim of this article is to provide a modeling of the second and third stage servo valves by comparison of the typical experimental reading and the computed curves obtained from simulation.

## 1 INTRODUCTION

The main difficulties of the modeling of an actuator hydraulic hexapod are servo valve models. In the case of electrical actuators operating in control voltage, the torque is got from the control voltage and the rotation speed of the motor. In the case of hydraulic actuator, for a current control of servo valve given, the efforts provided by the jack depend on the flow rate and consequently they depend also on the speed of the jack and leakages. This aspect is not taken into account by using the classical frequency model of the servo valve (Faisandier, 1999), (Mare, 2002), (Thayer, 1965).

At first, we will present the hydraulic model of the servo valve + jack system. In a second time, a nonlinear modeling will be developed. Lastly, the results obtained from the modeling will be presented and analyzed.

## 2 ELECTRO HYDRAULIC SYSTEM

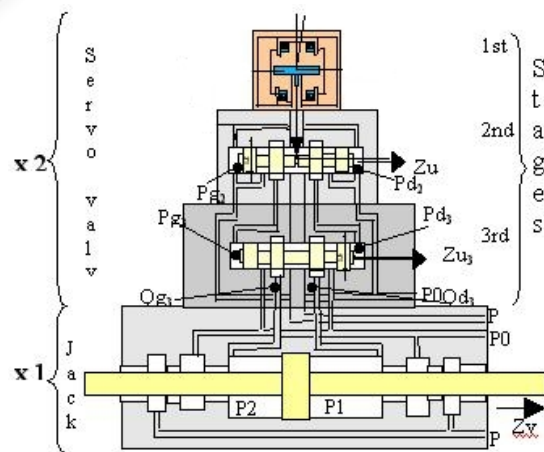


Figure 1: Diagrammatic section of system.

Figure 1 shows a model with three-stage servo valve and a jack. The symbol "x2" and "x1" indicate respectively the presence in the system of two

parallel servo valves supplying the jack. A servo valve is controlled by an electrical stage (1<sup>st</sup> stage), followed by a 2nd stage and a 3rd hydraulic amplification stage (Faisandier,1999), (Guillon, 1961).

A control current applied to the system input is named  $i$ . The double potentiometric hydraulic divisor of the first stage, leads to two pressures  $P_{g2}$  and  $P_{d2}$  applied to the end of the slide on the 2nd stage, the flow rates provided by this 2nd stage are named  $Q_{g2}$  and  $Q_{d2}$ , applied to the control of the slide displacement of the 3rd stage of the servo valve.

The third stage generates the flow rates  $Q_{g3}$  and  $Q_{d3}$  taking part in the sum of the flows entering and going out of the jack chambers, and leading, through instantaneous volumes of the chambers, and the compressibility coefficient of the oil, to the pressure variation in each chamber. The servo valve is supplied with pressure  $P_0$  and reservoir return line  $P$ .

### 3 MODELING

#### 3.1 Servo Valve Linear Model

Figure 2 shows linear diagram of a servo valve modeling (Pommier,2000).

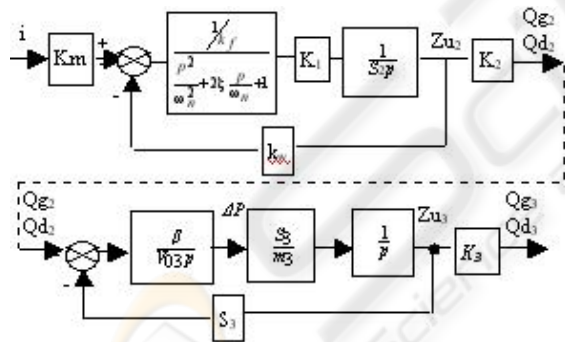


Figure 2: Linear diagram of the servo valve.

- $K_m$ : Gain between the current and the torque.
- $\omega_n$ : Undamped natural frequency of the pallet inertia of the 1st stage.
- $\zeta$ : Damping ratio of the friction of the pallet.
- $k_f$ : Gain displacement in torque of the nozzle pallet unit.
- $K_1$ : Gain in flow rate of hydraulic amplification.
- $S_2$ : Surface of the slide ends of the 2nd stage.
- $k_w$ : Gain of the feedback torque.
- $K_2$ : Gain in flow rate of the 2nd stage slide.
- $V_{03}$ : Effective volume when the slide is centered.
- $S_3$ : Surface of the slide ends of the 3rd stage.

- $m_3$ : Slide mass of the 3rd stage.
- $K_3$ : Gain in flow rate of the 3rd stage.

One notes that for this model, the  $K_2$  and  $K_3$  coefficients characterize the flow rate as a function of the slide positions. For the second stage, the  $K_2$  coefficient gives a good approximation within a large part of the operating area, contrary to the  $K_3$  coefficient suggesting that the speed of the jack does not depend on the load.

#### 3.2 Hydraulic Nonlinear Model

Figure 3 shows the general diagram describing the non-linear model of servo-valve-jack system.

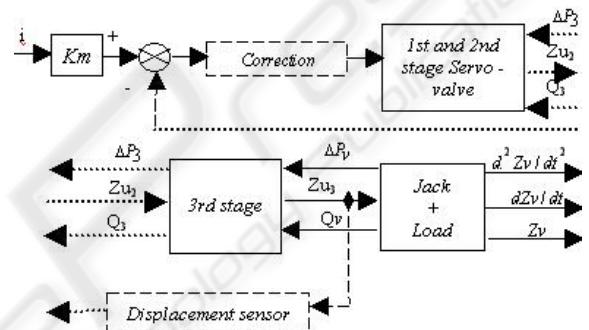


Figure 3: Nonlinear model of the servo valve + jack.

One takes into account the hydrodynamic forces applied to the various slides of the servo valves. These forces take part in the nonlinear behavior of the device. This functional diagram shows that the behavior of the servo valve and the jack cannot be dissociated and must be treated as such.

We have developed a nonlinear model of the servo-valve-jack unit allowing to determine, for a given control current, the effort supplied by the jack from the pressure variations within the control volumes formed by the jack chambers. This pressure variation after temporal integration defines the pressure within the right and left chambers of the jack. The difference of these pressures multiplied by the active section of the piston gives the effort supplied by the jack.

In our case, the main difficulty is the nonlinear modeling of the servo valve; more particularly we have to take into account a finite number of sensitive parameters and the hydraulic nonlinear behavior laws. In addition to the nonlinearities resulting from the hydraulic potentiometer, the pressure flow will be taken into account from the following relation:

$$Q = K \sqrt{\Delta P} \quad (1)$$

We assume that the flow rate of the fluid is viscous and incompressible, as turbulent type.

The transient flow rate associated with fluid incompressibility is proportional to the rate of change of pressure in a volume of control and may be expressed as:

$$(V/\beta)(dP/dt) + (dV/dt) = Q_e - Q_s \quad (2)$$

Where  $\beta$  is the bulk modulus of the fluid.

We also take into account the hydrodynamic forces on the various slides of the servo-valves, leading to the nonlinear behavior of the device.

$$F_{hd} = Q \sqrt{2(\gamma/g)} \quad (3)$$

Where  $\gamma$  is the specific gravity (kg/m<sup>3</sup>) and  $g$  is the gravitational acceleration.

The angular displacement of the frame engine versus the current is given by:

$$iKm + l\Delta P_2 - Kr_2LZu_2 = J\ddot{\theta} + \varphi\dot{\theta} + Kr_2L^2\theta + F_s \text{sign}(\dot{\theta}) \quad (4)$$

With  $\Delta P_2 = P_{g2} - P_{d2}$  difference of pressure between the two slide ends of the 2nd stage. From the equation (2) one can obtain the evolution laws of the pressures  $P_{g2}$  and  $P_{d2}$ .

$$\frac{dP_{g2}}{dt} = \frac{\beta}{V_{o2} + S_2Zu_2} \left( Q_{g1} - Q_b + Kf_2\sqrt{|P_0 - P_{g2}|} - S_2Zu_2 \right) \quad (5)$$

$$\frac{dP_{d2}}{dt} = \frac{\beta}{V_{o2} - S_2Zu_2} \left( Q_{d1} - Q_b + Kf_2\sqrt{|P_0 - P_{d2}|} + S_2Zu_2 \right) \quad (6)$$

Where,  $S_2Zu_2$  is the flow rate caused by the motion of the slide and  $Q_{g1}$  and  $Q_{d1}$  are the flow rates resulted from the pressure applied to the section of fixed openings  $S1$ ,  $Q_b$  is the flow rate from the nozzle tip.

By applying the fundamental principle of dynamics we obtain the sum of the forces applied to the slide of the 2nd stage:

$$S_2\Delta P_2 - Kr_2L\theta - F_{hd2} = m_2\ddot{Zu}_2 + \eta_2\dot{Zu}_2 + Kr_2Zu_2 + F_s \text{sign}(\dot{\theta}) \quad (7)$$

Where  $S_2\Delta P_2$  is the difference of forces applied to the ends of the slide,  $Kr_2L\theta$  is the force due to the stiffness and the deformation of the pallet.

The flow rate  $Q_{d2}$  and  $Q_{g2}$  provided by the 2nd stage is given by the equation (1). The equation of  $Q_{d2}$ ,  $Q_{g2}$  taking into account the slide covering and the resulting leakage. The modeling of the slide covering is exponential modeling, where  $\varepsilon$  is a constant. The very low value of  $\varepsilon$  ensures the continuity in the opening model of the slide and the leakage resulted from the slide covering.

From the equation (2), and (7), one can obtain the evolution laws of the pressures and the sum of the forces related to the third stage and the jack hydraulic.

## 4 IMPLEMENTATION AND RESULTS

At first, we have identified the parameters of the nonlinear model from the high-speed 5m/s servo-valve-jack unit of LAMEFIP laboratory. This first step gives us some experimental reference parameters for the validity of our servo-valve model.

The servo valve composed of the first and second stages and the second servo valve composed of the third stage are respectively hydaustar 550 and 1160 type servo valve. All the parameter values of the model estimated or measured of the electro hydraulic system for the second and third stages are summarized in table 1.

Table 1: Parameter values of the second and third stages.

Parameters		Manufacturer data	Estimated data
$L$	Length magnetic pallet	31.2e-3 (m)	-----
$l$	Outdistance between magnetic axis pallets and metering jets	10.5e-3 (m)	-----
$Dbuse$	Diameter of nozzle tip	0.18e-3 (m)	-----
$Sbuse$	Surface of nozzle tip	2.54e-8 (m <sup>2</sup> )	
$xo$	Length between magnetic axis pallets and metering jets	-----	55e-6 (m)
$Kbuse$	Gain of nozzle tip	-----	0.039 (m <sup>3</sup> /s/m)
$K1$	Gain of flow rate of the fixed section	-----	1.5e-9 (m <sup>3</sup> /s/m)
$Kf_2$	Gain of leakage in the stage	-----	5.15e-12 (m <sup>3</sup> /s/m)
$V_{o2}$	Volume control when the slide is centered	19.5e-9 (m <sup>3</sup> )	-----
$S_2$	Surface of slide	3.38e-5 (m <sup>2</sup> )	-----
$J$	Pallet inertia	-----	4e-7 (Kg m <sup>2</sup> )

$\Phi$	Viscous friction coefficient in rotation of the pallet	-----	$9e-4$ (Nm/rd s)
$K_{r2}$	Stiffness of the slide of the stage	2100 (N/m)	-----
$M_2$	Slide masse	$9e-3$ (Kg)	-----
$\psi_2$	Viscous friction coefficient in slide	-----	6 (Ns/m)
$K_{f3}$	Gain of leakage in the stage	-----	$1e-12$ ( $m^3/s/m$ )
$E$	Lap	-----	$3.7e-6$ (m)
$K_2$	Gain of flow rate of volume control in the stage	-----	$6e-4$ ( $m^3/s/m$ )
$S_3$	Surface of slide	$5e-4$ ( $m^2$ )	-----
$V_{O3}$	Volume control when the slide is centered	$8.6e-6$ ( $m^3$ )	-----
$M_3$	Slide masse	$276e-3$ (Kg)	-----
$\psi_3$	Viscous friction coefficient in slide	-----	1000 (Ns/m)

After completing the estimated parameters, we compare the typical experimental datas supplied by the manufacturer such as the flow rate – current characteristics for the second stage, the frequency response of the second and third stages with the curves resulting from the model using both the estimated values and the measured values.

#### 4.1 Flow Rate – Current Characteristics

We have compared the flow rate  $Qd2$  of the second stage of the servo valve under differential pressure of 70 bar when the current  $i$  varies in the range  $[-I_{max}; +I_{max}]$ ,  $I_{max}$  is the maximum value of the current modulus. The figure 4 shows the flow rate  $Qd2$  – current  $i$  characteristics for the 550 Hydraustar servo valve (second stage) supplied by the manufacturer and those obtained from the model.

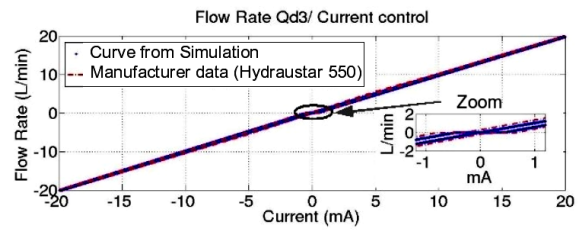


Figure 4: Flow rates / control currents characteristics supplied by manufacturer and those obtained from the model.

As shown in the figure 4, we can observe that the result obtained from the model and that provided by the manufacturer are similar when the current input reaches the maximal value of 20 mA. The maximal flow rate value provided by the driver servo valve reaches 20 l/min. One can observe the role of the leakages when the slide position is near the hydraulic zero as shown in the inset of the figure 4. These leakages result from the taking into account of the laps and the clearances between the slide and the sleeve. The figure 5 shows the computed flow rate  $Qd3$  of the third stage of the servo valve under differential pressure of 70 bar when the current varies from  $-I_{max}$  and  $+I_{max}$ . We obtain in this particular configuration, a maximal computed value of the flow rate provided by the servo valve of +/- 600 l/min. This value matches the manufacturer data for this servo valve model.

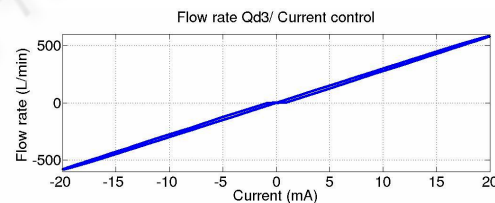


Figure 5: Flow rate  $Qd3$ / control current characteristics obtained by simulation.

#### 4.2 Frequency Response

We have compared the characteristic curves obtained from the bench test measurement (by using a servo valve flow with normalized decreasing of the pressure of 70 bar for different input levels) with the curves computed from our model.

##### 4.2.1 First and Second Stage

The figure 6 shows the comparison of the manufacturer curves with those obtained from the model for the similar operating conditions: provided

pressure  $P_s = 210$  bar, differential pressure 70 bar, 100% nominal current.

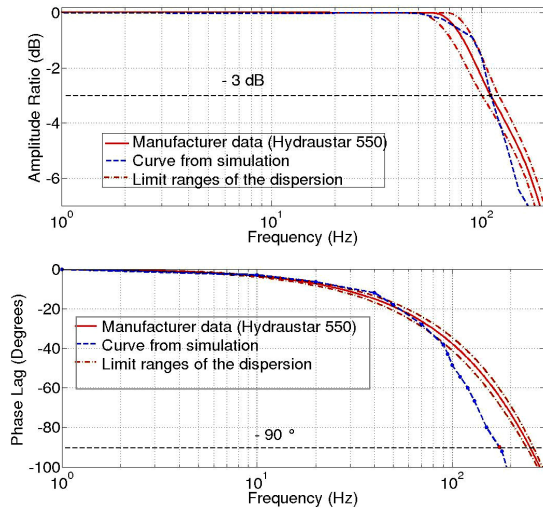


Figure 6: Frequency response for 100% of the nominal current. (for -3 dB,  $110 \text{ Hz} < f < 130 \text{ Hz}$ ,  $-90^\circ$ ,  $230 \text{ Hz} < f < 250 \text{ Hz}$ , theoretical curve).

The frequency response corresponding to 100 % of nominal current obtained from the model gives a cut-off frequency of 115 Hz for a gain of  $-3$  dB and a frequency of 180 Hz for a phase lag of  $90^\circ$ . The cut-off frequency for  $-3$  dB obtained with the model is in the limit range of the dispersion of frequencies provided by the manufacturer. For phase lag of  $90^\circ$ , the frequency error between both curves is estimated from 20% to 28 %.

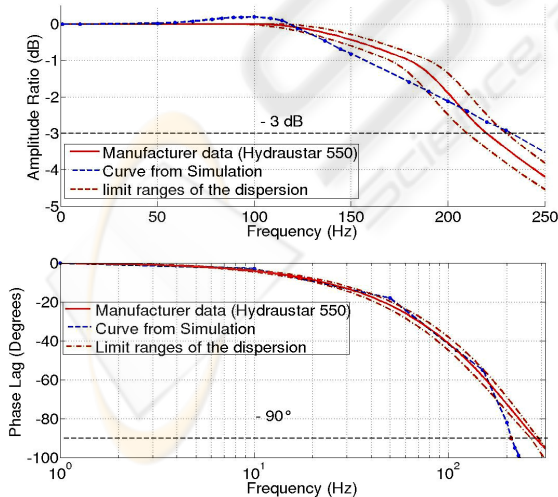


Figure 7: Frequency response for 25 % of the nominal current. (for  $-3$  dB,  $210 \text{ Hz} < f < 230 \text{ Hz}$  and for  $-90^\circ$ ,  $250 \text{ Hz} < f < 280 \text{ Hz}$ , theoretical curve).

The figure 7 shows the frequency comparison of the manufacturer curves and those obtained with the model for the similar operating conditions: Provided pressure  $P_s = 210$  bar, pressure difference 70 bar, 25 % of the nominal current.

The frequency response for 25% of the nominal current obtained from the model gives us a cut-off frequency of 220 Hz for a gain of  $-3$  dB and a frequency of 210 Hz for a phase lag of  $90^\circ$ . The cut-off frequency corresponding to a gain of  $-3$  dB is in the limit range of the dispersion of the manufacturer frequencies. The frequencies related to the phase lag of  $90^\circ$  obtained by modeling and those provided by manufacturer are different. The error is estimated from 16 % to 25 %. The computed curve shapes for the second stage are different from those supplied by the manufacturer. This difference should depend directly on the estimated values of the pallet inertia and its friction coefficient. An infinitesimal variation of these values leads to the under damping observed in amplitude plot of the bode diagram.

#### 4.2.2 Third Stage

We compare the frequency responses of the serial servo valve 1160, corresponding to the third stage, with the coupling of the serial servo valve 550 related to the driving stage. The figure 8 shows the typical response supplied by the manufacturer for 100 % of the nominal input signal.

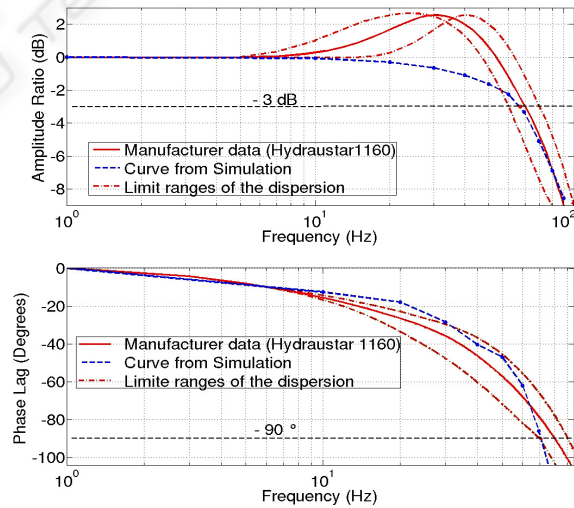


Figure 8: Frequency response for 100 % of the nominal current.

The driving servo valve is provided with a pressure  $P_s$  of 210 bar. The cut-off frequencies in the limit ranges of the dispersion for a frequency response corresponding to 100 % of the nominal

current match respectively 70 Hz and 85 Hz for  $-3$  dB and phase lag  $90^\circ$  for flow rates Qd3 and Qg3 of 600 l/min.

The frequency response for 100 % of the nominal value of the current obtained from the model gives a cut-off frequency of 70 Hz corresponding to a gain of  $-3$  dB and a frequency of 73 Hz for a phase lag of  $90^\circ$ . One observes that the results obtained for the servo valves corresponding to the second and third stages from the model and those supplied by the manufacturer are close. Nevertheless, one can note that a difference between the curves amplitude from the manufacturer and those obtained from the model. Indeed, the manufacturer curves show an under damping probably caused by the implementation of the corrector in the system whereas we have performed the modeling without corrections in loop control.

## 5 CONCLUSION

In our work, one can note that the servo valve is the limiting element of the servo valve + jack system. The flow rate values (20 l/min and 600 l/min provided by the second and the third stage respectively), like the bandwidth values of the driving servo valve corresponding to the second stage and those of the amplification stage e.g. the third stage, obtained from the model and supplied by manufacturer are rather similar. These results suggest that the estimated values, which cannot be measured, such as the gap  $x_0$  between the nozzle and the pallet, the inertia  $J$  and the viscous friction coefficients of the pallet  $\Phi$ , the friction coefficients of the slides  $\Psi_2, \Psi_3$  and the flow rate gains  $Kbuse, K1, Kf_2, K2, Kf_3$ , are fairly close to the physical values of the type 550 and 1160 Hydraustar servo valve. We have shown that the nonlinear model presented in this work have allowed us the accurate simulation of the nonlinear behavior of three stage servo valves between the current input and the flow rate output. This model allows the taking into account of the pressure into the jack chambers as a function of the forced stress. Hence with this model is possible to computed the dynamic and static behavior, the latter corresponds to the short circuit generated by jack stoppers.

At this stage, the interfacing with the SimMecanics software, by introducing as input this corresponding to the effort between two "bodies", the quantity  $(P1-P2)Sp$  ( $Sp$ : useful piston surface), will provide as output from the software, the speed and the relative position of both bodies.

## ACKNOWLEDGEMENTS

Special thanks go to Mr. Terrade (Hydraustar company) for supplying technical support.

## REFERENCES

- Faisandier, J., 1999. *Mécanismes hydrauliques et pneumatiques*, 8<sup>e</sup> édition, Paris, Dunod.
- Mare, J.C., 2002, *Actionneurs Hydrauliques*, Commande . Techniques de l'ingénieurs, traité l'informatique industrielle.S731.
- Thayer, W.J., 1965, *Transfer functions for moog servo valves*, Technical bulletin 103, MOOG INC. Springer-Verlag.
- Guillon, M., 1961, *Etude et détermination des systèmes hydrauliques*, Paris, Dunod.
- Pommier, V., Lanusse P., Oustaloup A., 2000, *Commande CRONE d'un actionneur hydraulique*. In Journée Franco-Tunisiennes, Monastir, Tunisie.